

# Transformation of Dion–Jacobson-type layered oxyfluorides into new anion-deficient pyrochlore-type oxides, $\text{ASrNb}_2\text{O}_{6.5}$ (A = Li and Na)

Jong-Young Kim, In Chung, Seung-Joo Kim and Jin-Ho Choy\*

National Nanohybrid Materials Laboratory, School of Chemistry and Molecular Engineering, College of Natural Sciences, Seoul National University, Seoul 151–747, Korea.

E-mail: jhchoy@plaza.snu.ac.kr; Fax: +82–2–872–9864; Tel: +82–2–880–6658

Received 9th August 2001, Accepted 24th January 2002

First published as an Advance Article on the web 4th March 2002

New pyrochlore-type oxides,  $\text{ASrNb}_2\text{O}_{6.5}$  (A = Li and Na), were prepared from Dion–Jacobson-type layered perovskite oxyfluorides,  $\text{ASrNb}_2\text{O}_6\text{F}$ . The prototype layered perovskite phases are transformed into anion-deficient pyrochlore-type oxides by heating above 600 °C in air. The  $\text{ASrNb}_2\text{O}_6\text{F}$  (A = Rb and K) and  $\text{RbCaNb}_2\text{O}_6\text{F}$  compounds have the layered perovskite structure, whereas the pyrochlore structure is found to be more stable than the layered perovskite in the  $\text{AF–SrNb}_2\text{O}_6$  (A = Li and Na) and  $\text{KF–CaNb}_2\text{O}_6$  systems.

## Introduction

A number of  $\text{A}_2\text{B}_2\text{O}_7$  and  $\text{AA'BB'O}_7$  oxides have been reported to adopt the pyrochlore structure, which originates from the mineral of  $\text{NaCa}(\text{Nb,Ta})_2\text{O}_6(\text{OH/F})$ . As pointed out by Subramanian *et al.*, the structural stabilities of the pyrochlore-type  $\text{A}_2\text{B}_2\text{O}_7$  (A = rare earth, B = transition metal) oxides can be determined from the radius ratio of the A and B cations.<sup>1,2</sup> As shown by  $\text{Sr}_2\text{Ta}_2\text{O}_7$ ,  $\text{Sr}_2\text{Nb}_2\text{O}_7$ , and  $\text{La}_2\text{Ti}_2\text{O}_7$ , when the A/B ratios are relatively large, the layered perovskite structure is more stable than the pyrochlore structure.<sup>3</sup>

Recently, we have been able to synthesize new ion-conducting oxyfluorides,  $\text{ASrNb}_2\text{O}_6\text{F}$  (A = Li, Na, and Rb), with a Dion–Jacobson-type layered perovskite structure.<sup>4</sup> It has been also found that these 2-dimensional layered perovskite oxyfluorides compete with 3-dimensional pyrochlore-type oxides. In the present study, we attempted to synthesize new pyrochlore-type oxides,  $\text{Li}(\text{Na})\text{SrNb}_2\text{O}_{6.5}$ , from layered perovskite oxyfluorides,  $\text{Li}(\text{Na})\text{SrNb}_2\text{O}_6\text{F}$ , and to investigate their crystal structures by X-ray diffraction analyses. Furthermore, the relative structural stabilities of the pyrochlore and the layered perovskite phases for  $\text{A}(\text{Sr/Ca})\text{Nb}_2\text{O}_6\text{F}$  (A = Li, Na, K, and Rb) have been systematically studied.

## Experimental

The layered perovskite-type compounds  $\text{RbSr}(\text{Ca})\text{Nb}_2\text{O}_6\text{F}$  and  $\text{KSrNb}_2\text{O}_6\text{F}$  were prepared by heating stoichiometric mixtures of  $\text{Sr}(\text{Ca})\text{Nb}_2\text{O}_6$  and  $\text{RbF/KF}$  at 750 °C in a sealed gold tube filled with highly purified  $\text{N}_2$  gas.<sup>4</sup> The compound  $\text{KCaNb}_2\text{O}_6\text{F}$ , prepared by the reaction of  $\text{CaNb}_2\text{O}_6$  and  $\text{KF}$  in a Au tube, was found to have a pyrochlore-type structure.

The Li and Na derivatives,  $\text{Li}(\text{Na})\text{SrNb}_2\text{O}_6\text{F}$ , with a layered perovskite structure, were obtained by the ion-exchange reaction of  $\text{Rb}(\text{K})\text{SrNb}_2\text{O}_6\text{F}$ .<sup>4</sup> After heating these Li and Na derivatives at 600 °C for 24 h in air, the pyrochlore-type oxides,  $\text{Li}(\text{Na})\text{SrNb}_2\text{O}_{6.5}$ , could be obtained (Figs. 1 and 2). In addition, the  $\text{Li}(\text{Na})\text{SrNb}_2\text{O}_6\text{F}$  compounds were heated at 600 °C in a sealed Au tube filled with  $\text{N}_2$  gas in order to compare the relative stability of the layered perovskite and

pyrochlore structures, which produced pyrochlore phases and minor impurities ( $\text{LiNbO}_3$ ,  $\text{NaNbO}_3$ , *etc.*) (Fig. 3).

Powder XRD patterns were recorded in reflection mode

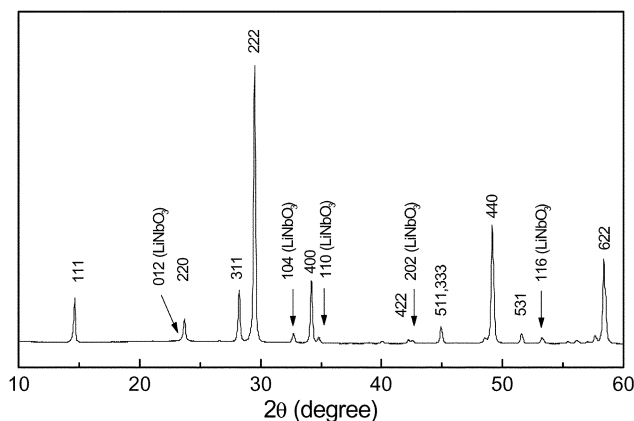


Fig. 1 X-Ray diffraction profile for  $\text{LiSrNb}_2\text{O}_{6.5}$ .

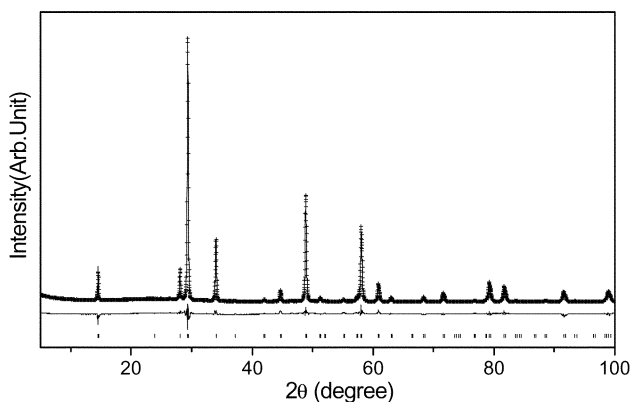
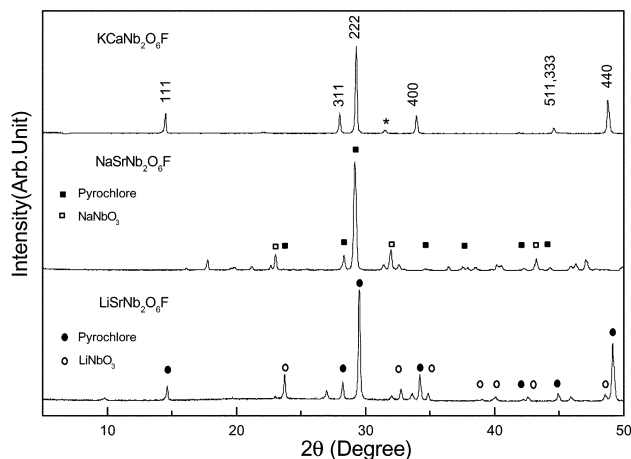
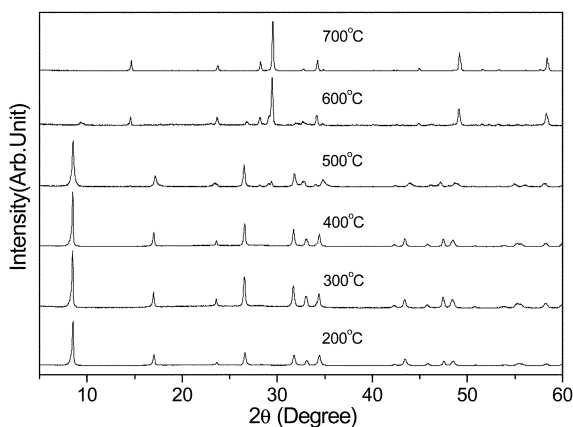


Fig. 2 X-Ray diffraction profiles for  $\text{NaSrNb}_2\text{O}_{6.5}$ : calculated (solid line), observed (cross), difference (bottom solid line), and Bragg position (vertical mark underneath) are presented.



**Fig. 3** X-Ray diffraction patterns for the solid-state reaction products formed by heating  $\text{ASrNb}_2\text{O}_6\text{F}$  ( $A = \text{Li}$ , and  $\text{Na}$ ) and  $\text{KF} + \text{CaNb}_2\text{O}_6$  in a sealed Au tube filled with an  $\text{N}_2$  atmosphere. The asterisk indicates an unknown impurity.



**Fig. 4** Temperature-dependent XRD patterns for  $\text{LiSrNb}_2\text{O}_6\text{F}$ .

using a Philips PW 3710 diffractometer with  $\text{Cu-K}\alpha$  radiation. Data were collected in the step scan mode with counts for 5 s at  $0.02^\circ$  interval. Detailed crystallographic parameters were derived from Rietveld refinement using the RIETAN-94 program.<sup>5</sup> Thermogravimetric analyses (TG and DSC) were carried out on a Rigaku TAS-100 thermobalance. Sample weights were about 30 mg and thermal runs were performed in air at a rate of  $5 \text{ K min}^{-1}$ .

## Results and discussion

### Crystallographic analyses of the pyrochlore phases

The crystal structures for  $\text{Rb(K)SrNb}_2\text{O}_6\text{F}$  and their ion-exchange derivatives  $\text{Li(Na)SrNb}_2\text{O}_6\text{F}$  are analogous to those for  $\text{Rb(K)LaNb}_2\text{O}_7$  and  $\text{Li(Na)LaNb}_2\text{O}_7$ , respectively.<sup>6–8</sup> As shown in the temperature-dependent XRD patterns (Fig. 4),  $\text{LiSrNb}_2\text{O}_6\text{F}$  transforms into a pyrochlore-type phase ( $\text{LiSrNb}_2\text{O}_{6.5}$ ) and  $\text{LiNbO}_3$ <sup>9</sup> beyond  $500^\circ\text{C}$ . Fig. 5 shows that Na oxyfluoride also turns into the pyrochlore-type  $\text{NaSrNb}_2\text{O}_{6.5}$  at  $600^\circ\text{C}$ . As for  $\text{RbSrNb}_2\text{O}_6\text{F}$ , Rb-oxyfluoride is decomposed into  $\text{RbSr}_2\text{Nb}_3\text{O}_{10}$  and minor impurities above  $600^\circ\text{C}$  (Fig. 6).

Such structural transformations are consistent with the results of thermal analyses. As shown in Figs. 7 and 8, exothermal peaks are observed at  $540$  and  $600^\circ\text{C}$  for the Li and Na compounds, respectively, which correspond to the transition temperatures from the layered perovskite to the pyrochlore structure. For  $\text{LiSrNb}_2\text{O}_6\text{F}$ , the theoretical weight loss

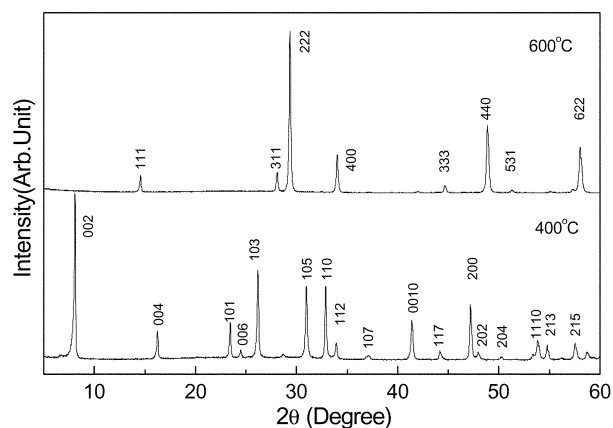


**Fig. 5** Temperature-dependent XRD patterns for  $\text{NaSrNb}_2\text{O}_6\text{F}$ .

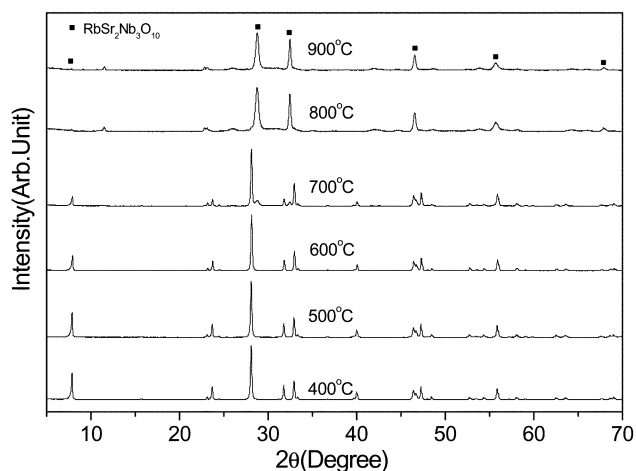


**Fig. 6** Temperature-dependent XRD patterns for  $\text{RbSrNb}_2\text{O}_6\text{F}$ .

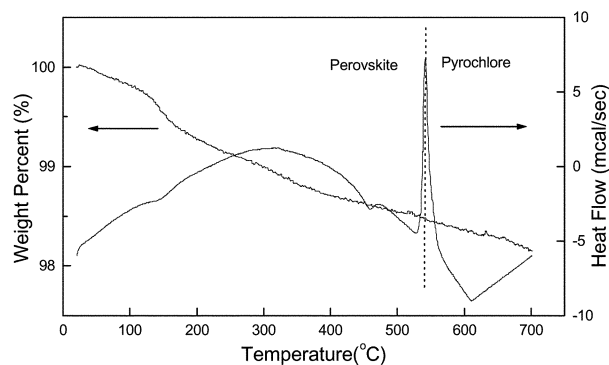


**Fig. 7** Thermogravimetric (TG and DSC) analyses for  $\text{LiSrNb}_2\text{O}_6\text{F}$ .

due to the volatilization of fluorine should be about 2.7%. However, the experimental weight loss is calculated to be about 1.9%. Thermal decomposition in the TGA measurements was thought to be unsaturated, which is probably due to the fast thermal scan rate ( $5^\circ\text{C min}^{-1}$ ) compared to the decomposition reaction. For the purposes of XRD measurements and the preparation of  $\text{LiSrNb}_2\text{O}_{6.5}$ ,  $\text{LiSrNb}_2\text{O}_6\text{F}$  was heated at  $600^\circ\text{C}$  for 24 h in air. The reaction was thus fully saturated and, therefore, fluorine and unreacted impurities are absent. We recorded the  $^{19}\text{F}$  NMR spectrum for the Li-pyrochlore phase, which showed no signal for fluorine. The large weight loss up to  $300^\circ\text{C}$  for  $\text{NaSrNb}_2\text{O}_6\text{F}$  ( $\sim 6\%$ ) is due to the presence of interlayer water. As-prepared  $\text{NaSrNb}_2\text{O}_6\text{F}$  is very hygroscopic and immediately forms a hydrated phase in ambient

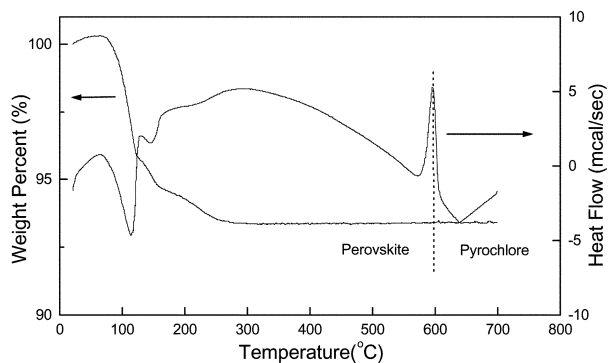


Fig. 8 Thermogravimetric (TG and DSC) analyses for NaSrNb<sub>2</sub>O<sub>6</sub>F.

Table 1 Crystallographic data for pyrochlore-type NaSrNb<sub>2</sub>O<sub>6.5</sub><sup>a</sup>

Atom	Site	<i>g</i>	<i>x</i>	<i>y</i>	<i>z</i>	<i>B</i> /Å <sup>2</sup>
Na/Sr	16c	1.0	0.0	0.0	0.0	1.0(4)
Nb	16d	1.0	0.5	0.5	0.5	0.1(3)
O(1)	48f	1.0	0.408(5)	1/8	1/8(2)	3.3(15)
O(2)	8a	0.5	1/8	1/8	1/8	3.3(15)

<sup>a</sup>Space group: *Fd3m*, *a* = 10.5324(2) Å, *R*<sub>wp</sub> = 15.64, *R*<sub>p</sub> = 11.76, *S* = *R*<sub>wp</sub>/*R*<sub>c</sub> = 6.5718, *R*<sub>t</sub> = 9.57, and *R*<sub>f</sub> = 8.88, unit cell volume = 1168.37 Å<sup>3</sup>, calculated density = 4.55 g cm<sup>-3</sup>, interatomic distances (Å) Nb–O, 2.10(2); Na/Sr–O(1), 2.50(3); Na/Sr–O(2), 2.28(0).

conditions.<sup>4</sup> The hydrated phase shows larger interlayer spacing than the dehydrated one. From <sup>19</sup>F MAS NMR spectra for the thermally-treated Na sample (600 °C for 24 h in air), it was also found that the fluorine atoms are absent in such samples.

All the peaks in the XRD pattern for the Li phase (Fig. 1) can be successfully indexed using cubic pyrochlore and a small amount of LiNbO<sub>3</sub> (~10%). The unit cell parameter is calculated to be 10.4771(2) Å on the basis of cubic symmetry. As stated above, NaSrNb<sub>2</sub>O<sub>6</sub>F with a layered perovskite structure also turns into NaSrNb<sub>2</sub>O<sub>6.5</sub> with a pyrochlore structure after thermal treatment at 600 °C. Rietveld refinement of the pyrochlore phase was carried out with the cubic pyrochlore model (space group: *Fd3m*).<sup>10,11</sup> The calculated profiles of NaSrNb<sub>2</sub>O<sub>6.5</sub> are presented in Fig. 2 together with the observed and difference patterns. The refinement results and the selected bond lengths are presented in Table 1.

### Competition between the layered perovskite and the pyrochlore-type structures

RbSr(Ca)Nb<sub>2</sub>O<sub>6</sub>F and KSrNb<sub>2</sub>O<sub>6</sub>F, which were prepared by solid-state reaction of RbF/KF + Sr(Ca)Nb<sub>2</sub>O<sub>6</sub>, have the layered perovskite structure (ref. 4 and Fig. 9). As expected, their crystal structures are analogous to those for RbLaNb<sub>2</sub>O<sub>7</sub> and KLaNb<sub>2</sub>O<sub>7</sub>.<sup>4,7,8</sup> By contrast, the solid-state reaction of KF + CaNb<sub>2</sub>O<sub>6</sub> in a sealed Au tube yields the pyrochlore-type oxide with minor impurities (Fig. 3). The crystallographic data for RbCaNb<sub>2</sub>O<sub>6</sub>F, KSrNb<sub>2</sub>O<sub>6</sub>F, and KCaNb<sub>2</sub>O<sub>6</sub>F are summarized in Table 2.

Unlike ASrNb<sub>2</sub>O<sub>6</sub>F (*A* = K and Rb) and RbCaNb<sub>2</sub>O<sub>6</sub>F, the (Li/Na)F + SrNb<sub>2</sub>O<sub>6</sub>, (Li/Na)F + CaNb<sub>2</sub>O<sub>6</sub>, and KF + CaNb<sub>2</sub>O<sub>6</sub> systems have different structures depending on the

Table 2 Crystallographic data for (Rb/K)(Sr/Ca)Nb<sub>2</sub>O<sub>6</sub>F

Atom	Structure	Symmetry	<i>a</i> /Å	<i>b</i> /Å	<i>c</i> /Å
RbSrNb <sub>2</sub> O <sub>6</sub> F <sup>4</sup>	Layered perovskite	Tetragonal	3.8503(1)		11.2841(3)
RbCaNb <sub>2</sub> O <sub>6</sub> F <sup>a</sup>	Layered perovskite	Orthorhombic	7.6029(2)	7.6229(2)	22.0154(5)
KSrNb <sub>2</sub> O <sub>6</sub> F	Layered perovskite	Orthorhombic	3.8606(3)	22.286(2)	3.8489 (3)
KCaNb <sub>2</sub> O <sub>6</sub> F	Pyrochlore	Cubic	10.558 (3)		

<sup>a</sup>Extended unit cell (*a'* ~ 2*a*, *b'* ~ 2*b*, *c'* ~ 2*c*).

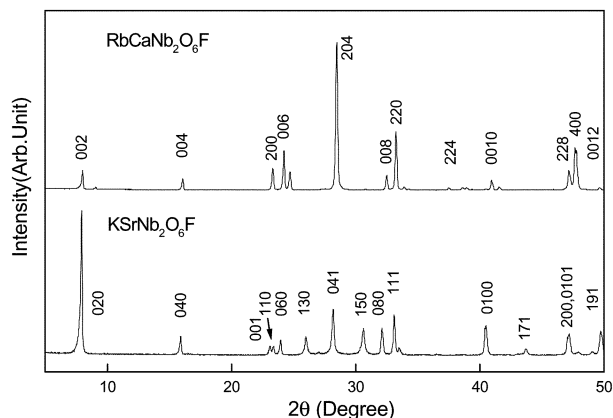


Fig. 9 X-Ray diffraction patterns for RbCaNb<sub>2</sub>O<sub>6</sub>F and KSrNb<sub>2</sub>O<sub>6</sub>F obtained by solid-state reaction in an N<sub>2</sub> atmosphere.

synthetic method used. The Li, Na, and K derivatives, prepared by ion-exchange reaction of the Rb form, maintain their parent layered perovskite structure. In contrast, the Li and Na ion-exchange derivatives transform into the pyrochlore-type oxides, such as Li(Na)SrNb<sub>2</sub>O<sub>6.5</sub>, on thermal treatment in air (Figs. 1 and 2). Furthermore, heating the layered perovskite-type (Li/Na)SrNb<sub>2</sub>O<sub>6</sub>F in a closed, inert system (Au tube filled with N<sub>2</sub> gas) at 600 °C, produced pyrochlore phases with minor impurities (Fig. 3). In the same manner, direct solid-state reaction of KF + CaNb<sub>2</sub>O<sub>6</sub> yields the pyrochlore phase and a minor impurity (Fig. 3). These results show that the layered structure is thermodynamically metastable and that the pyrochlore structure is more stable in the (Li/Na)F + SrNb<sub>2</sub>O<sub>6</sub>, (Li/Na)F + CaNb<sub>2</sub>O<sub>6</sub>, and KF + CaNb<sub>2</sub>O<sub>6</sub> systems.

It has been pointed out in earlier studies<sup>1,2</sup> that the structural stabilities of the pyrochlore phase in R<sub>2</sub>M<sub>2</sub>O<sub>7</sub> ternary oxides (*R* = rare earth; *M* = transition metal) are determined by the size ratio *R*/*M*, which is also applicable to the present system, A(Sr/Ca)Nb<sub>2</sub>O<sub>6</sub>F. When the *A* cations are relatively small, such as Li (0.92 Å for 8-fold coordination) and Na (1.18 Å), the ionic radius ratios for (*A*/Sr) and Nb, *R*<sub>(A/Sr)/R<sub>Nb</sub></sub>, are 1.70 and 1.90 for the Li and Na compounds, respectively. As for ACaNb<sub>2</sub>O<sub>6</sub>F, the *R*<sub>(A/Ca)/R<sub>Nb</sub></sub> values are 1.59 and 1.80 for the Li and Na derivatives, respectively. In these Li and Na compounds, the pyrochlore-type oxides are more stable than the layered perovskite-type oxyfluorides.

In the case of larger *A* cations such as Rb (1.61 Å) and K (1.51 Å), the *R*<sub>(A/Sr)/R<sub>Nb</sub></sub> values are 2.31 and 2.16 for RbSrNb<sub>2</sub>O<sub>6</sub>F and KSrNb<sub>2</sub>O<sub>6</sub>F, respectively, and the Dion–Jacobson-type layered perovskite structure is more stable than the pyrochlore structure. RbCaNb<sub>2</sub>O<sub>6</sub>F (*R*<sub>(Rb/Ca)/R<sub>Nb</sub></sub> = 2.13) also has a layered perovskite structure. In contrast, KCaNb<sub>2</sub>O<sub>6</sub>F [*R*<sub>(K/Ca)/R<sub>Nb</sub></sub> = 2.05] adopts the pyrochlore-type structure. Therefore, it is thought that the pyrochlore-type structure is dominant over the layered perovskite when the *R*<sub>A/R<sub>B</sub></sub> ratio is smaller than about 2.10 in A<sub>2</sub>B<sub>2</sub>X<sub>7</sub>-type oxides or oxyfluorides (Table 3). These results are consistent with earlier results for (RNa)(TiNb)O<sub>6</sub>F (*R* = Ce, Pr, Nd, Eu, Gd, Yb, and Y).<sup>2</sup> In these pyrochlore-type oxyfluorides, the *R*<sub>(R/Na)/R<sub>(Ti/Nb)</sub></sub> values are calculated to be 1.866–1.739.

**Table 3** Relationship between the  $R_{(A/Ca)}/R_{Nb}$  or  $R_{(A/Sr)}/R_{Nb}$  values and the crystal structures in the  $A(Sr/Ca)Nb_2O_6F$  system ( $A = Li, Na, K,$  and  $Rb$ )<sup>a</sup>

	A cation							
	Li		Na		K		Rb	
	Ca	Sr	Ca	Sr	Ca	Sr	Ca	Sr
$R_{(A/Sr)}/R_{Nb}$ or $R_{(A/Ca)}/R_{Nb}$	—	1.70	—	1.90	2.05	2.16	2.13	2.31
Structure	—	Pyro	—	Pyro	Pyro	Perov	Perov	Perov

<sup>a</sup>Pyro = pyrochlore structure. Perov = layered perovskite structure.

## Conclusion

The structural transformation of Dion–Jacobson-type layered perovskite oxyfluorides,  $ASrNb_2O_6F$  ( $A = Li$  and  $Na$ ), into the pyrochlore-type oxides,  $ASrNb_2O_{6.5}$  ( $A = Li$  and  $Na$ ), has been reported. Temperature-dependent XRD patterns and thermogravimetric analyses (TG and DSC) show that the prototype layered perovskite phases turn into anion-deficient pyrochlore oxides above 600 °C. In the  $A(Sr/Ca)Nb_2O_6F$  ( $A = Rb, K, Na,$  and  $Li$ ) system, the relative structural stability of the pyrochlore and the layered perovskite phases is found to be dependent on the ratio of the ionic radius of  $[A/(Sr/Ca)]$  and  $Nb$ . When the  $R_{[A/(Sr/Ca)]}/R_{Nb}$  value is lower than about 2.10, the pyrochlore-type structure is more stable than the layered perovskite.

## Acknowledgement

The authors wish to acknowledge fellowships from the Ministry of Education (Brain Korea 21 program) and the Ministry of Science and Technology (National Research Laboratory 1999).

## References

- 1 M. A. Subramanian, G. Aravamudan and G. V. Subba Rao, *Prog. Solid State Chem.*, 1983, **15**, 55.
- 2 M. A. Subramanian and A. W. Sleight, *Handbook on the Physics and Chemistry of Rare Earths*, Vol. 16, Elsevier, New York, 1993.
- 3 (a) N. Ishizawa, F. Marumo, T. Kawamura and M. Kimura, *Acta Crystallogr., Sect. B: Struct. Crystallogr. Cryst. Chem.*, 1976, **32**, 2524; (b) N. Ishizawa, F. Marumo, T. Kawamura and M. Kimura, *Acta Crystallogr., Sect. B: Struct. Crystallogr. Cryst. Chem.*, 1975, **31**, 1912; (c) M. Gasperin, *Acta Crystallogr., Sect. B: Struct. Crystallogr. Cryst. Chem.*, 1975, **31**, 2129.
- 4 J. H. Choy, J. Y. Kim, S. J. Kim, J. S. Sohn and O. H. Han, *Chem. Mater.*, 2001, **13**, 906.
- 5 F. Izumi, in *Rietveld Method*, ed. R. A. Young, Oxford University Press, Oxford, 1993, ch. 13.
- 6 A. R. Armstrong and P. A. Anderson, *Inorg. Chem.*, 1994, **33**, 4366.
- 7 J. Gopalakrishnan and V. Bhat, *Mater. Res. Bull.*, 1987, **22**, 412.
- 8 M. Sato, J. Abo, T. Jin and M. Ohta, *J. Alloys Compd.*, 1993, **192**, 81.
- 9 H. D. Megaw, *Acta Crystallogr., Sect. A: Cryst. Phys., Diffr., Theor. Gen. Cryst.*, 1968, **24**, 583.
- 10 T. Takeda, R. Kanno, Y. Kawamoto, M. Takano, F. Izumi, A. W. Sleight and A. W. Hewat, *J. Mater. Chem.*, 1999, **9**, 215.
- 11 I. Radosavljevic, J. S. O. Evans and A. W. Sleight, *J. Solid State Chem.*, 1998, **136**, 63.